Journal of Hydraulic Research

ISSN: 0022-1686 (Print) 1814-2079 (Online) Journal homepage: https://www.tandfonline.com/loi/tjhr20

Coherent structures in flow over hydraulic engineering surfaces

Ronald J. Adrian & Ivan Marusic

To cite this article: Ronald J. Adrian & Ivan Marusic (2012) Coherent structures in flow over hydraulic engineering surfaces, Journal of Hydraulic Research, 50:5, 451-464, DOI: 10.1080/00221686.2012.729540

To link to this article: https://doi.org/10.1080/00221686.2012.729540

Copyright Taylor and Francis Group, LLC

Published online: 10 Oct 2012.

Submit your article to this journal

Article views: 4092

View related articles

Citing articles: 28 View citing articles

Full Terms & Conditions of access and use can be found at
https://www.tandfonline.com/action/journalInformation?journalCode=tjhr20

IAHR AIRH
Taylor & Francis
Taylor & Francis Group

Journal of Hydraulic Research Vol. 50, No. 5 (2012), pp. 451–464
http://dx.doi.org/10.1080/00221686.2012.729540
© 2012 International Association for Hydro-Environment Engineering and Research

Vision paper

Coherent structures in flow over hydraulic engineering surfaces

RONALD J. ADRIAN, Ira A. Fulton Professor, *School for Engineering of Matter, Transport and Energy, Arizona State University, Tempe, AZ 85287, USA.*
Email: rjadrian@asu.edu (author for correspondence)

IVAN MARUSIC, Professor, *Department of Mechanical Engineering, University of Melbourne, Victoria 3010, Australia.*
Email: imarusic@unimelb.edu.au

ABSTRACT
Wall-bounded turbulence manifests itself in a broad range of applications, not least in hydraulic systems. Here, we briefly review the significant advances over the past few decades in the fundamental study of wall turbulence over smooth and rough surfaces, with an emphasis on coherent structures and their role at high Reynolds numbers. We attempt to relate these findings to parallel efforts in the hydraulic engineering community and discuss the implications of coherent structures in important hydraulic phenomena.

Keywords: Coherent structures; Reynolds number effects; roughness; wall turbulence

1 Introduction

Flows over surfaces in hydraulic engineering are almost always intensely turbulent, owing to the low viscosity of water and the characteristically large scales of length, δ_0, and mean flow velocity, U. The archetypes for this class of flows are steady mean motions over smooth, flat surfaces with large fetch, for example, turbulent boundary layers or internal wall flows such as those in pipes and channels.

Classically, understanding of these flows is based largely on the average behaviour of the important aspects of the flow such as mean velocity and mean wall-shear stress, τ_w. The mean velocity exhibits at least in two different layers, an *inner layer* in which the wall-shear stress, expressed in terms of the friction velocity, $u_\tau = \sqrt{\tau_w/\rho}$, and the kinematic viscosity, ν, are the important external parameters; and an *outer layer* in which the depth of the flow δ_0 (equal to the boundary layer thickness δ, the pipe radius R or channel depth h) and the free stream velocity U_∞ or the bulk velocity U_b determine the average behaviour of the mean velocity profile. These layers share a common part, the *logarithmic* layer, in which the mean velocity varies logarithmically with distance from the wall, y. Coles' logarithmic plus wake formulation (Coles 1956) gives the mean velocity in the outer layer according to

$$U^+ \equiv \frac{U(y)}{u_\tau} = \kappa^{-1}\ln(y^+) + A + \Pi W(y/\delta_0), y^+ > 30 \quad (1)$$

where von Kármán's constant, $\kappa \cong 0.41$ and $A \cong 5$ are empirical constants, and *Coles' wake factor* Π is an empirical, non-dimensional parameter that depends upon the free stream pressure gradient. The empirical fit $W \approx \sin^2(y/\delta_0)$ describes the deviation of the mean velocity from the logarithmic variation in the so-called *wake region*, and $y^+ = yu_\tau/\nu$ is the distance from the wall in units of the *viscous length scale*, ν/u_τ. The logarithmic variation dominates for $y \leq 0.15\delta_0$, nominally.

The mean velocity in the inner layer is described classically by von Kármán's logarithmic law above $y^+ \cong 30$, and a viscously dominated *buffer layer* for $0 \leq y^+ \leq 30$. (Modern investigations suggest that the mean velocity does not vary logarithmically until higher values, $y^+ \geq 200$ in boundary layers (Nagib *et al.* 2007) and 600 in pipes (Zagarola and Smits 1998), but for the purposes of this discussion, it suffices to use $y^+ = 30$ for reference.) Thus, the logarithmic layer nominally exists between

$$\frac{30}{\mathrm{R}_\tau} < \frac{y}{\delta_0} < 0.15 \quad (2)$$

Revision received 10 September 2012/Open for discussion until 30 April 2013.

ISSN 0022-1686 print/ISSN 1814-2079 online
http://www.tandfonline.com

where

$$\mathsf{R}_\tau \equiv \frac{u_\tau \delta_0}{\nu} = \delta_0^+ \tag{3}$$

can be interpreted either as a turbulent Reynolds number or as the ratio of the layer depth to the viscous length scale, known as the *von Kármán number*.

Neo-classically, there has been considerable research effort to understand the behaviour of the flow statistics in terms of structural elements, variously called *motions, coherent structures* or *eddies* (Townsend 1976, Cantwell 1981, Hussain 1986). Coherent motions are recurrent, persistent motions that characterize the flow and play important roles in determining mean flow, stress and other statistical properties. They may have rotational and irrotational parts. Eddies are similar, but in the spirit of Townsend (1976) they are definitely rotational. Further discussion can be found in Marusic and Adrian (2013), but for the present purposes it suffices to think of coherent structures as building blocks of flows that are recognizable, despite randomness, by their common topological patterns, and that occur over and over again.

The quantitative validity of the logarithmic variation of the mean velocity and the scaling laws that pertain to it have been questioned (Barenblatt 1993), especially for boundary layers (George and Castillo 1997), but there is now no doubt (Smits *et al.* 2011) that the logarithmic law continues to be one of the cornerstones of wall turbulence, and that the physics of the logarithmic region play a central role in the overall fluid mechanics of wall turbulence. This role extends to important issues such as the proper boundary conditions for Reynolds-averaged Navier–Stokes equations and large eddy simulations, and to the asymptotically infinite Reynolds number structure of the eddies of wall turbulence.

Despite the clear importance of the logarithmic layer at high Reynolds number and over a variety of surfaces, surprisingly little of our knowledge about the structures of eddies within the logarithmic layer is used in the treatment of hydraulic wall flows. For example, it is well known that the logarithmic law can be derived by postulating that the mixing length grows in proportion to y, and that it varies qualitatively as shown in Fig. 1(a). This proportionality in the logarithmic layer is consistent with Townsend's *Attached Eddy Hypothesis*, which states that the eddies in wall turbulence have sizes that are proportional to their distance from the wall (Fig. 1b). But, very little else about the geometry of the eddies, their origin or their dynamics is used in the classical hydraulic engineering literature.

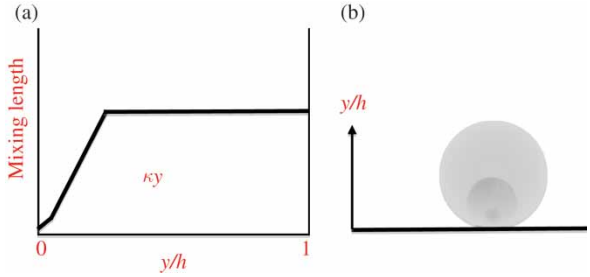

Figure 1 (a) Classical mixing length profile; (b) schematic illustration of Townsend's attached eddy hypothesis in which the attached eddies grow in size in proportion to their distance from the wall

The place of understanding coherent structures within the hydraulics research portfolio is developing, and its ultimate applications remain to be established. Certainly, understanding how structures create motions that transport momentum, energy and scalars can be expected to materially improve the ability to predict average behaviour. Further, understanding the component structures of a turbulent flow is also likely to provide a conceptual framework within which observations of hydraulic phenomena can be assessed. Lastly, understanding the coherent structures may make the design of hydraulic structures easier.

The purpose of this "vision paper" is to summarize what is known about the structure of coherent structures in wall turbulence, especially the high Reynolds number turbulence of hydraulic flow applications, and to offer some ideas on the significance of the structures in problem areas such as sedimentation, erosion and flow–structure interactions. Throughout, we shall relate the coherent structures to the known regions of the mean velocity profile, as discussed above.

2 Coherent structures on smooth walls

2.1 *Near-wall structures*

Before considering rough and irregular surfaces, it is valuable to consider the large body of work done on hydrodynamically smooth surfaces. Particularly, as theory (Townsend 1976, Jimenez 2004) indicates that for roughness length scales less than a few percent of the boundary layer thickness, the logarithmic and fully outer regions are not affected by roughness, apart from setting the inner boundary condition for the friction velocity, u_τ.

The coherent structures that occur in the near-wall portion of the inner layer have been extensively reviewed by Kline (1978), Cantwell (1981), Hussain (1986), Robinson (1991), Adrian (2007) and others. Many characteristic elements have been recognized and documented in the near-wall layer, including: low-speed streaks with spacing of 100 viscous wall units and the burst process (Kline *et al.* 1967), sweeps and ejections (Brodkey *et al.* 1974), quasi-streamwise vortices, Q2/Q4 events (Wallace *et al.* 1972, Willmarth and Lu 1972) and associated variable integration time average (VITA) events (Blackwelder and Kaplan 1976) and inclined shear layers (Kim 1987). Here, Q2/Q4 refers to events in the second and fourth quadrants of the $u - v$ map, which thus contribute a positive contribution to the Reynolds shear stress, $-\overline{uv}$. It is noted here that we define u and v as the fluctuating components of velocity in the streamwise and wall-normal directions, respectively. The bursting process in the near-wall region, in which low-speed fluid is ejected abruptly away from the wall, is considered to play an important role in the overall dynamics of the boundary layer.

Different interpretations exist as to what type of coherent structures exist and what role they play in the near-wall region, and many of these viewpoints are reviewed by Robinson (1991), Panton (2001), Schoppa and Hussain (2002), Adrian (2007), Marusic *et al.* (2010b) and Jimenez (2012). Here, we emphasize the hairpin vortex as a simple coherent structure that explains many of the features observed in the near-wall layer (Theodorsen 1952, Head and Bandyopadhyay 1981), or its more modern, and demonstrably more common variant, the asymmetric hairpin or the cane vortex (Guezennec *et al.* 1989, Robinson 1991, Carlier and Stanislas 2005). For brevity, we shall not distinguish between symmetric and asymmetric hairpins, nor will we distinguish between hairpins and horseshoes, since available evidence suggests that these structures are variations of a common basic structure at different stages of evolution or in different surrounding flow environments. In this regard, it may be also useful to group all such eddies into the class of *turbines propensii* (referring to "inclined eddies") to de-emphasize the connotations of shape that are intrinsic to the term "hairpin".

Theodorsen's (1952) analysis considered perturbations of the spanwise vortex lines of the mean flow that were stretched by the shear into intensified hairpin loops. Smith (1984) extended this model and reported hydrogen bubble visualizations of hairpin loops at low Reynolds number. While there is evidence for a formation mechanism like Theodorsen's in homogeneous shear flow (Rogers and Moin 1987, Adrian and Moin 1988), it is clear that Theodorsen's model requires modification near a wall to include long quasi-streamwise vortices spaced about 50 viscous wall units apart and connected to the head of the hairpin by vortex necks inclined at roughly 45° to the wall (Robinson 1991). With this simple model, the low-speed streaks are explained as the viscous sub-layer, low-speed fluid that is induced to move up from the wall by the quasi-streamwise vortices. A schematic illustrating these essential features of a hairpin vortex is shown in Fig. 2. The second quadrant ejections are the low-speed fluid that is caused to move through the inclined loop of the hairpin by vortex induction from the legs and the head, and the VITA event is the stagnation point flow that occurs when the Q2 flow through the hairpin loop encounters a Q4 sweep of higher speed fluid moving towards the back of the hairpin. This part of the flow constitutes the inclined shear layer. This picture is substantiated by the direct experimental observations of Liu *et al.* (1991), who used particle image velocimeter (PIV) to examine the structure of wall turbulence in the streamwise wall-normal plane of a fully developed low Reynolds number channel flow. They found shear layers growing up from the wall which were inclined at angles less than 45° from the wall. Regions containing high Reynolds stress were associated with these near-wall shear layers. Typically, these shear layers terminate in regions of rolled-up spanwise vorticity, which could be the heads of hairpin vortices. In the near-wall hairpin model, ejections are associated with the passage of hairpin vortices.

Perhaps the strongest experimental support for the existence of hairpin vortices in the logarithmic layer was originally given by Head and Bandyopadhyay (1981), who studied high-speed, time-sequenced, images of smoke-filled boundary layers over a large Reynolds number range. They concluded that the turbulent boundary layer consists of hairpin structures that are inclined at a characteristic angle of 45° to the wall. Head and Bandyopadhyay (1981) also proposed that the hairpins occur in groups whose heads describe an envelope inclined at 15–20° with respect to the wall. The picture is similar to Smith's (1984)

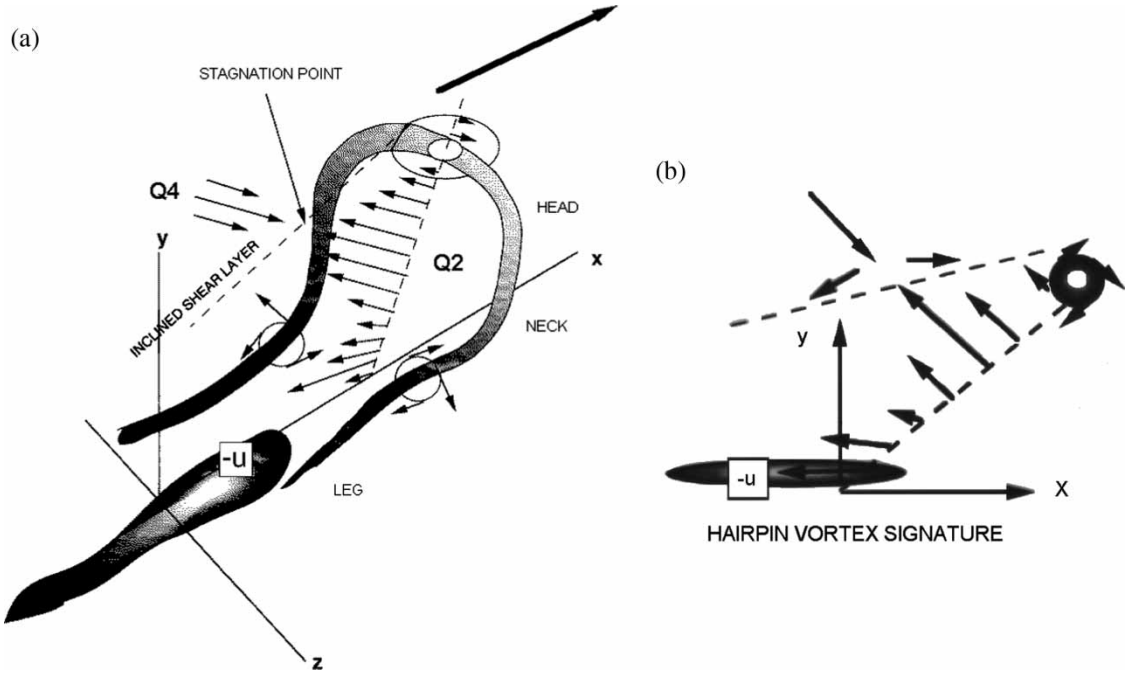

Figure 2 Schematic of hairpin eddy attached to the wall; (b) signature of the hairpin eddy in the streamwise/wall-normal plane (from Adrian *et al.* 2000)

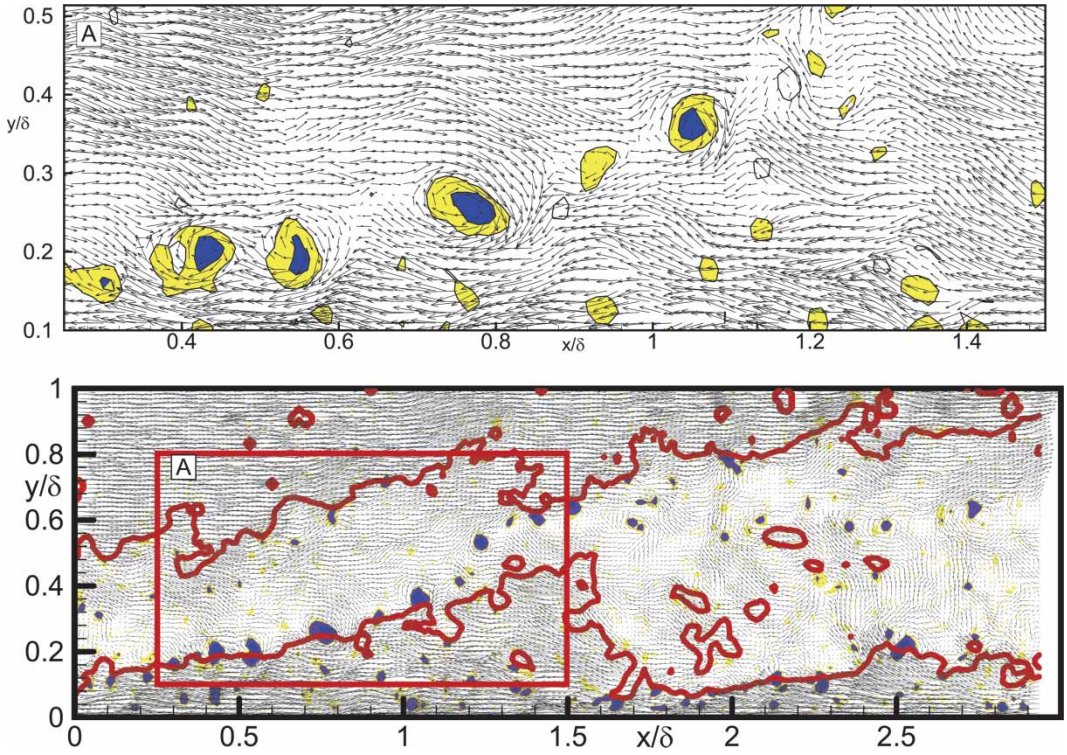

Figure 3 PIV measurements of the velocity field and vorticity field (coloured contours) in a turbulent boundary layer flowing left to right. The ramp-like structures bounded by groups of concentrated vorticies are evidence of hairpin vortex packets in which hairpins occur in a streamwise alignment with smaller, upstream hairpins auto-generated by larger, downstream hairpins. The velocity fields magnified in the upper inset figure posses the characteristics of hairpins identified in Figure 2 (from Adrian *et al.* 2000)

interpretation of flow visualizations in water, but instead of being based on data below $y^+ = 100$, Head and Bandyopadhyay (1981) appear to have based their construct on direct observations of ramp-like patterns on the *outer* edge of the boundary layer (Bandyopadhyay 1980), plus more inferential conclusions from data within the boundary layer. The observations of Head and Bandyopadhyay (1981) led Perry and Chong (1982), with later refinements by Perry *et al.* (1986) and Perry and Marusic (1995), to develop a mechanistic model for boundary layers based on Townsend's (1976) attached eddy hypothesis where the statistically representative attached eddies are hairpin vortices.

An important aspect of the attached eddy modelling work is that a logarithmic region requires a range of scales to exist with the individual eddies scaling with their distance from the wall. However, achieving such a range of scales requires a sufficiently high Reynolds number, which makes measurements difficult due to the large dynamic range required. A major advance in this regard came with the development of high-resolution PIV. Adrian *et al.* (2000) were the first to extensively use PIV to study the logarithmic and fully outer regions of boundary layers over a range of Reynolds numbers. Their work was particularly important as the PIV measurements provided images of the distribution of vorticity and the associated induced flow patterns without invoking the inferences needed to interpret flow visualization patterns. The patterns revealed that the logarithmic region is characterized by spatially coherent packets of hairpin vortices, with a range of scales of packets coexisting. This scenario explained the observed inclined regions of uniform momentum where the interfaces of these regions coincided with distinct vortex core signatures. A sample instantaneous PIV result is shown in Fig. 3. The "attached" hairpin packet scenario explains, or at least is consistent with a number of observations made in turbulent boundary layers. For example, it explains the observation that the spacing of the low-speed streaks in the streamwise velocity fields increases across the logarithmic region with distance from the wall (Ganapathisubramani *et al.* 2003, 2005, Tomkins and Adrian 2005). Moreover, if one associates a burst with a packet of hairpins, this construct offers an explanation both for the long extent of the near-wall low-speed streaks and for the occurrence of multiple ejections per burst, which has been documented in a number of studies (Bogard and Tiederman 1986, Luchik and Tiederman 1987, Tardu 1995). Thus, the original conception of a turbulent burst being a violent eruption in time is replaced by a succession of ejections due to the passage of a packet of hairpin vortices, the smallest hairpin creating the strongest ejection velocity.

2.2 *Large-scale motions and very large-scale superstructures*

Flow visualizations of boundary layers, an example of which is shown in Fig. 4, highlight that in the outer layer, the edge of the turbulent zone has bulges that are about 2–3δ long (Kovasznay *et al.* 1970) separated by deep crevasses between the back of one bulge and the front of another (Cantwell 1981). The backs have stagnation points formed by high-speed fluid sweeping

Figure 4 Flow visualization of a turbulent boundary layer. Flow is from left to right and the visualization details are as described in Cantwell *et al.* (1978). Photo courtesy of Don Coles

downward, and the shear between the high-speed sweep and the lower speed bulge creates an inclined, δ-scale shear layer. The bulges propagate at about 80–85% of the free stream velocity.

Long streamwise lengths are also prominent in streamwise velocity energy spectra, as reported by Balakumar and Adrian (2007). They showed that two large length scales emerge in pipe, channel and boundary layer flows where one peak in energy is associated with large-scale motions (LSMs) of typical length 2–3δ, and a second longer wavelength peak is associated with very-large-scale motions (VLSM), or superstructures, on the order of 6δ for boundary layers (Hutchins and Marusic 2007a). On the basis of the shapes of the streamwise power spectra and the *uv* co-spectra, Balakumar and Adrian (2007) nominally placed the dividing line between LSM and VLSM at 3δ. Using this demarcation, Balakumar and Adrian (2007) showed that the LSM wavelength persists out to about $y/\delta \sim 0.5$ (consistent with the observed bulges in visualizations), while the very large superstructure wavelengths do not extend beyond the logarithmic region, ending at approximately $y/\delta = 0.2$.

While the reported lengths for the very large superstructure events from spectra are approximately 6δ for boundary layers, this is considerably less than the observed values in pipe and channel flows (Kim and Adrian 1999, Monty *et al.* 2007, 2009), suggesting that geometrical confinement issues may play a role. However, what the actual lengths of the very large superstructures are remains an open question. Hutchins and Marusic (2007a) used time-series from a spanwise array of hot-wires (and sonic anemometers in the atmospheric surface layer) to infer lengths well in excess of 10δ, and this is consistent with the high-speed PIV study of Dennis and Nickels (2008). Sample results of

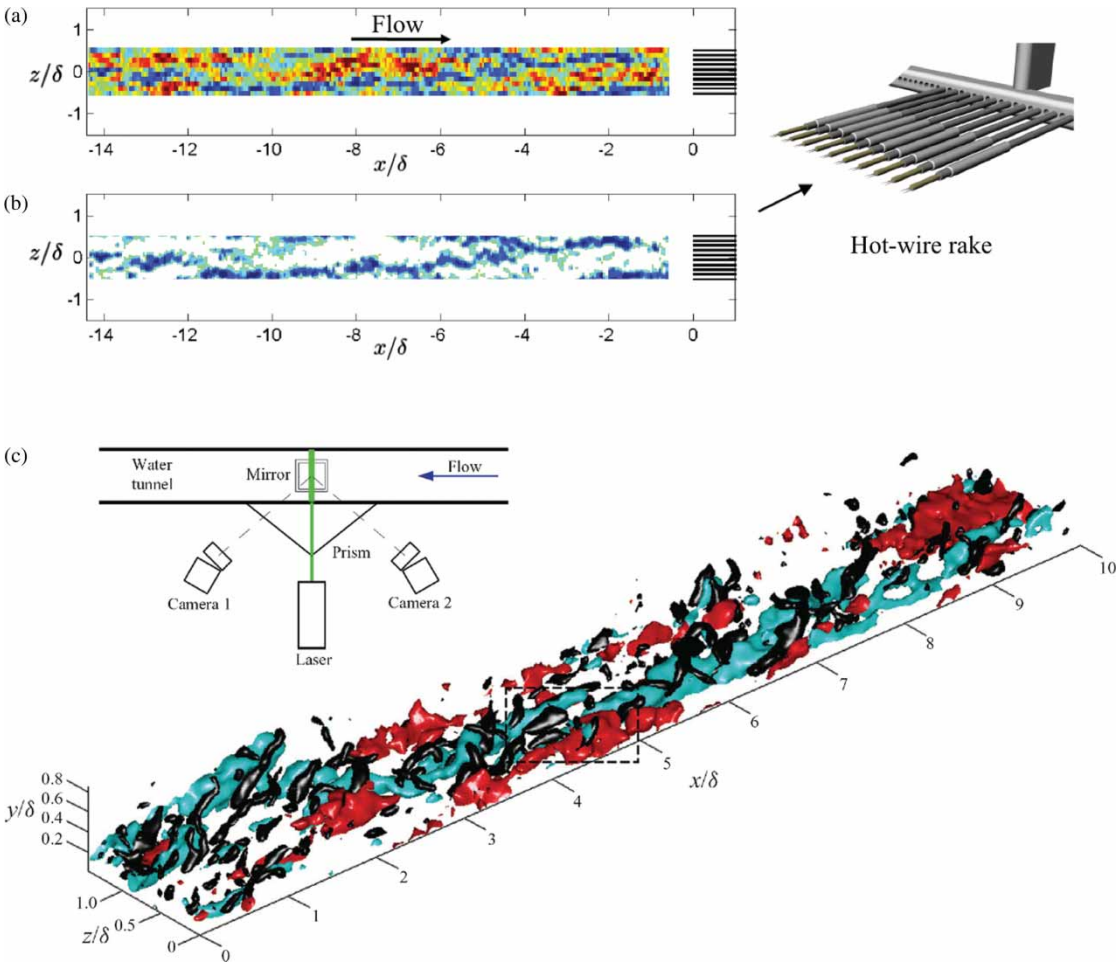

Figure 5 Very large-scale superstructure signatures: (a) from rake of hot-wire traces from Hutchins and Marusic (2007a); *u* signal at $y/\delta = 0.15$ for $R_\tau = 14,400$. (b) Same with only low-speed regions highlighted. (c) High-frame rate stereo-PIV measurements from Dennis and Nickels (2011a, b) in a turbulent boundary layer at $R_\delta = 4700$, showing similar features to the hot-wire rake measurements. Here, the black isocontours show swirl strength, indicating the corresponding location of vortical structures with the low-speed (blue) and high-speed (red) regions. After Marusic and Adrian (2013)

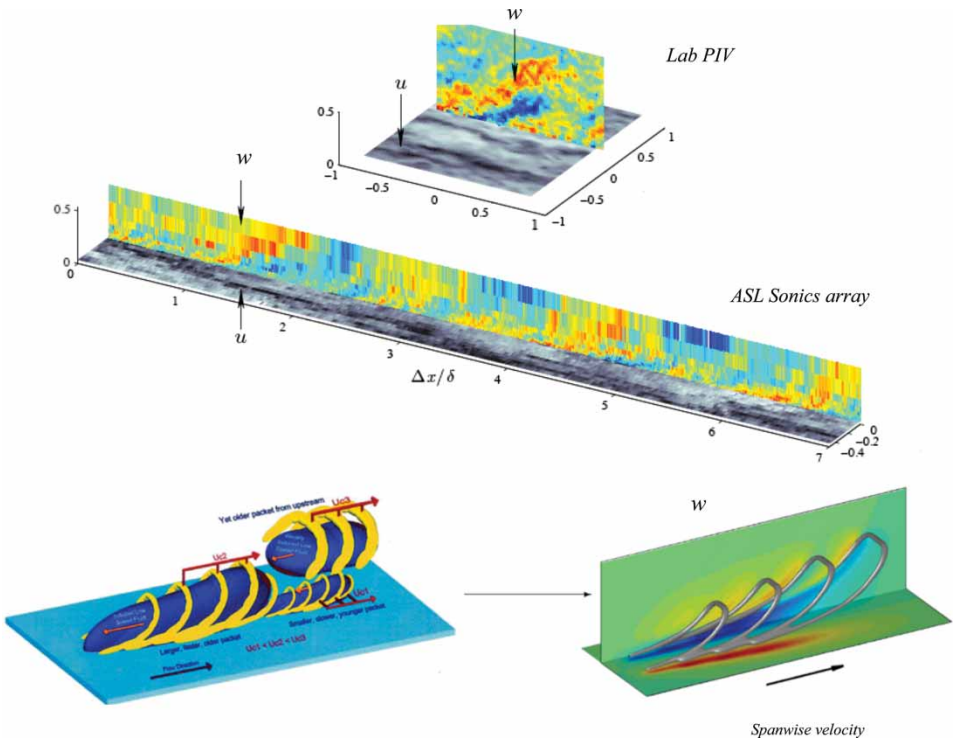

Figure 6 Top panel: instantaneous velocity fluctuations in the streamwise-wall-normal (x–y) plane and instantaneous streamwise velocity fluctuations in the streamwise/spanwise (x–y) planes for data from laboratory PIV (Hambleton *et al.* 2006) and for the atmospheric surface layer using an arrays of sonic anemometers (Hutchins *et al.* 2012). High-positive w regions are indicated by red, while blue denotes highly negative w regions. High-negative u regions are indicated by dark grey, while light grey shade denotes highly positive u regions. Bottom panel shows the Biot Savart law calculations for an idealized packet of hairpin vortices with their image vortices in the wall, as per the schematic of Adrian *et al.* (2000) shown on the left side

instantaneous measurements from Hutchins and Marusic (2007a) and Dennis and Nickels (2011a) are shown in Fig. 5.

The Dennis and Nickels (2011a,b) results also shed invaluable information on the three-dimensional structure of the largest motions, and while not conclusive, strongly support the suggestion by Kim and Adrian (1999) that the very large superstructures are a result of a concatenation of packets. Support for this also comes from atmospheric surface layer and laboratory measurements as described in Hambleton *et al.* (2006) and Hutchins *et al.* (2012), as shown in Fig. 6, where simultaneous $x-y$ and $x-z$ plane three-component velocity measurements reveal signatures entirely consistent with the superstructure events consisting of an organized array of packet structures. The lower schematics in Fig. 6 indicate comparisons with the Adrian *et al.* (2000) packet paradigm with Biot–Savart calculations of an idealized packet of hairpin vortices to infer what the corresponding spanwise velocity signatures would be in the relevant orthogonal planes.

2.3 *Interactions across scales*

An important consequence of the large-scale and very large superstructure motions in the outer region (which includes the logarithmic region) is their role in interacting with the inner near-wall region, including their influence on the fluctuating wall-shear stress. There has been debate over many decades as to whether the inner and outer regions do interact, or whether they can be considered as independent, as assumed in all classical scaling approaches. Considerable evidence now exists that outer scales are important for characterizing near-wall events. This stems from a large number of studies that have documented a Reynolds number (or equivalently an outer length scale) dependence in the near-wall region. These include the studies of Rao *et al.* (1971), Blackwelder and Kovasznay (1972), Wark and Nagib (1991), Hunt and Morrison (2000), DeGraaff and Eaton (2000), Metzger and Klewicki (2001), Abe *et al.* (2004), Hoyas and Jimenez (2006), Hutchins and Marusic (2007a), Orlu and Schlatter (2011) and others. Many of the above studies support the viewpoint that some superposition of the LSMs is experienced right to the wall. Hutchins and Marusic (2007b) went further and proposed that this interaction also involved a modulation of the large scales on the near-wall small-scale motions. Previous suggestions of modulation effects have also been made by Grinvald and Nikora (1988). Mathis *et al.* (2009) studied the modulation effect extensively using data over a large range of Reynolds number and showed that the degree of modulation increased with increasing Reynolds number, and hence is a key aspect of high Reynolds number wall turbulence.

Marusic *et al.* (2010a) extended the observations of a superposition and modulation of the large-scale outer motions in the near-wall region to a predictive model, whereby a statistically representative fluctuating streamwise velocity signal near the wall could be predicted given only a large-scale velocity signature from the logarithmic region of the flow. The model was shown to work well over a large Reynolds number range

for various statistics, including higher order moments. The formulation involves a universal signal and universal parameters, which are determined from a once-off calibration experiment at an arbitrarily chosen (but sufficiently high) Reynolds number. Marusic *et al.* (2011) further extended the model to predict the fluctuating wall-shear stress given only a large-scale streamwise velocity signal from the logarithmic region, and were able to reproduce the empirical result of Alfredsson *et al.* (1988) and Orlu and Schlatter (2011) that showed that the standard deviation of the inner-scaled fluctuating wall-shear stress increases as a logarithmic function of the Reynolds number.

3 Effect of high R in hydraulic engineering

The significance of the logarithmic layer depends on the Reynolds number. At low Reynolds number, most of the change of the velocity from the wall to the free-stream occurs from the wall to the top of the viscous-inertial buffer layer because the thickness of the logarithmic layer is small, and there is relatively little change in the velocity in the wake region. For example, in turbulent channel flow at Reynolds number $\mathsf{R}_\tau = 180$ (corresponding to $U_b h/\nu = 2800$), the mean velocity at the edge of the buffer layer is approximately 75% of the centreline velocity, and the velocity change across the logarithmic layer is very small. If one interprets the skin friction coefficient as a quantity that specifies the free stream velocity corresponding to a given level of wall shear stress, the foregoing consideration indicates that over half of the skin friction coefficient is determined by the fluid mechanics of the buffer layer at low Reynolds number, and hence that drag reduction strategies must concentrate on modifying the flow in the buffer layer. This view is supported by the fact that the rate of production of turbulent kinetic energy per unit volume, $-\overline{uv}\partial U/\partial y$, achieves a large maximum within the buffer layer, while it is much smaller in the logarithmic layer, suggesting that the preponderance of the turbulence is created in the buffer layer at low Reynolds number.

However, at high Reynolds numbers these conclusions must be altered substantially, simply because the logarithmic layer becomes much thicker, and thereby becomes more important. Consider for the sake of estimation equation (1). The velocity change from the wall to the top of the buffer layer is 13.2 friction velocities, while the velocity change from the top of the buffer layer to the top of the log layer (using $y/\delta_0 = 0.15$) is $2.41 \ln \delta^+ - 12.8$. The ratio of the velocity rise across the logarithmic layer to the velocity rise across the buffer layer is $0.183 \ln \delta^+ - 0.97$, implying that the velocity change across the buffer layer vanishes as $\approx 5.5/\ln \delta_0^+$ for large Reynolds number. Thus, as Reynolds number becomes infinite, essentially all of the velocity change occurs across the logarithmic layer, and hence all of the skin friction is associated with the logarithmic layer.

Practically, this conclusion is too strong, because the logarithmic dominance increases very slowly. For example, for 90% of the velocity change from the wall to the top of the logarithmic layer to occur across the logarithmic layer, the Kármán number must exceed 10^{23}, far above the value achieved by any terrestrial flow. On the other hand, for typical Reynolds number laboratory flows (say, $\delta^+ = 2000$), the velocity changes across the buffer layer, logarithmic layer and wake region are nominally 50, 25 and 25% of the free stream velocity, respectively. Thus, the logarithmic layer does not dominate laboratory flows, but its contribution is very substantial.

Similar conclusions can be drawn regarding the contribution that the logarithmic layer makes to the total production of the turbulent kinetic energy. For example, while the production per unit volume does peak in the buffer layer, the volume of the logarithmic layer is much greater, so the ratio of the production integrated over the logarithmic layer to the total production from within the buffer layer grows as $\ln y^+$ as Reynolds number approaches infinity. They are equal at approximately $\delta_0^+ = 35,000$.

Considerations such as the foregoing plus others have led Smits *et al.* (2011) to conclude that a reasonable criterion for wall turbulence to be considered high Reynolds number is $\delta_0^+ > 13,300$ for boundary layers and $\delta_0^+ > 50,000$ for pipe flow. These values are achieved commonly in hydraulic flows, so it is safe to assert *that nearly all hydraulic flows are high Reynolds number wall turbulence*. (For example, the turbulent Reynolds number of a boundary layer in a water flow with a free stream velocity of 2.5 m/s and a depth of 1 m is approximately 100,000.) This simple rule implies that hydraulic wall turbulence:

1. Possesses a clear range of logarithmic behaviour in the mean velocity profile and a clear range of $k^{-5/3}$ behaviour in the inertial sub-range of the power spectrum of the streamwise velocity.
2. Has larger production of turbulent kinetic energy in the logarithmic layer than in the buffer layer.
3. Possess a spectral peak at very long wavelengths that is distinct from the spectral peak corresponding to the inner layer motions.

With regard to the coherent structures, high Reynolds number implies ample room for eddies to grow from their initially small scales at the wall to the depth of the flow. The range of scales in the outer layer increases as $\delta^+/100$, if we take 100 viscous wall units as the representative height of the smallest first-generation hairpin and δ as the tallest coherent structure. If attention is confined to the self-similar structures in the logarithmic layer, the scale ratio is approximately $0.15\delta^+/100 = 150$ at $\mathsf{R}_\tau = 100,000$, making room for at least seven doublings of the original height of the smallest hairpin ($100 \times 2^7 = 12,800 < 15,000$). This implies seven or more different uniform momentum zones across the logarithmic layer.

4 Roughness effects on coherent structure

The surfaces bounding hydraulic flows are seldom smooth, and the height of the roughness elements can easily exceed the

thickness of the viscous buffer layer at the high Reynolds numbers of hydraulic flows. Roughness elements disrupt the flow within the buffer layer, and they may completely destroy it, replacing the effects of fluid viscosity with the effects of wall roughness and replacing the viscous length scale with the roughness element length scale, k (of course, a thin viscous sublayer is still attached to the surface of roughness elements, but its very small thickness makes it dynamically insignificant). A measure of the importance of the roughness elements is the non-dimensional roughness element height $k^+ = ku_\tau/\nu$. Small values of k^+ correspond to incomplete roughness, and large values correspond to complete or *fully developed* roughness. While roughness may destroy the viscous buffer layer, it appears to have much less effect on the logarithmic layer, other than shifting the effective slip velocity of the logarithmic layer with respect to the wall (Townsend 1976). The logarithmic law in Eq. (1) is, thus, replaced by

$$U^+ = \kappa^{-1} \ln y^+ + B(k^+) + \Pi W(y/\delta_0) \tag{4}$$

We shall refer to this phenomenon as *robustness of the logarithmic layer*. The persistence of the logarithmic layer implies that the under-lying structures, such as hairpins packets and related *turbines propensii* also persist. Their form need not be identical to the structures over smooth walls, but the evidence suggests that they are not very different (Hommema and Adrian 2003, Guala, *et al.* 2012). We, therefore, adopt, as a working hypothesis for now, the idea that *the structures in the outer layer of turbulent flow over rough walls having roughness elements that are smaller than the logarithmic layer are similar to those occurring in the outer layer of turbulent flow over smooth walls.*

If the roughness elements become a significant fraction of the logarithmic layer, they can severely disrupt the self-similar structures, and the logarithmic layer is replaced by different behaviour. A hint as to how this may happen is contained in the companion paper to this paper (Guala *et al.* 2012) in which tall hemispherical roughness elements are placed sparsely on an otherwise smooth surface. Measurements show two types of structures co-existing: hairpin packets from the smooth surface and hairpin packets from the individual hemispheres. The essential difference between the two types is that the latter grow at a steeper angle than the former and each of the latter packets is rooted to the hemisphere that generates it, much like wake vortices shed from a stationary cylinder. This behaviour hints at the effects that might be expected from rivets on the surfaces of marine vessels or very large roughness elements in streams and beds, such as large rocks.

5 Coherent structures and hydraulic phenomena

Turbulent transport plays a critical role in heat and mass transfer at the free surface, mixing and dispersion, erosion and sedimentation, inlet conditions to hydraulic devices, interaction with vegetation and, of course, resistance to flow. As such, insights into the coherent structures that influence transport provide new ways of looking at each of these phenomena (Nezu 2005, Nikora *et al.* 2007, Nikora 2010, Grant and Marusic 2011).

5.1 *Coherent structures in canonical open-channel flows*

Here, we consider flow in straight, wide channels of depth h with smooth walls, unless otherwise stated. The most obvious coherent feature of open-channel flow is the boil phenomena (Yalin 1992, Nezu and Nakagawa 1993). These localized, intense upwellings occur one after another in streaks along the streamwise direction with a spacing of approximately $2h$ (Tamburrino and Gulliver 1999), which corresponds, to the large-scale motions (bulges) in turbulent boundary layers. The streaks of boils coincide with streaks of low-speed flow, upwelling and lateral spreading at the surface. They are separated by streaks of high-speed flow lateral convergence and downwelling (Tamburrino and Gulliver 1999, 2007). From the upwelling and downwelling long, streamwise-oriented rolling vortices apparently first inferred by Velikaniv (1958; Shvidchenko and Pender 2001) and observed by many subsequent workers (Klaven and Kopaliani 1973 and more recently Tamburrino and Gulliver (1999, 2007), and Rodriguez and Garcia (2008) to cite a few).

The roll cells, also called large streamwise vortices (Gulliver and Halverson 1987) or long longitudinal eddies (Imamoto and Ishigaki 1986), look like secondary flows in the plane perpendicular to the streamwise flow (Nikora and Roy 2012). True secondary flows have non-zero long-time averages, and they affect the distribution of mean velocity, turbulence intensities, Reynolds shear stresses and bed shear stress throughout the channel. If the channel is wide enough, width $> 5h$, Nezu and Rodi (1986) observed that secondary flows are hard to see in the long-time averages, but they exist, nonetheless. PIV measurements of the cross-stream flow find cellular secondary currents that vary in time regardless of the aspect ratio (Onitsuka and Nezu 2001). This suggests that the long streamwise vortices meander in time as the aspect ratio increases, causing their features to be lost in time average measurements. Tamburrino and Gulliver (2007) observed that large-scale eddies having spanwise (lateral) widths of 1–1.5 h oscillate slowly in the mid channel, but fixed stationary secondary flows form in the vicinity of the side walls. Nezu and Nakayama (1997) observe both secondary currents and time-varying cellular currents in the interaction between the mainstream and a flood plain. Correlation measurements of the streamwise surface velocity made in many rivers indicate positive correlation over 2–5h followed by negative correlation between 5 and 10h, and finite correlation, either positive or negative over lengths extending to 10–20h (Sukhodolov *et al.* 2011). The oscillating sign of the correlation in Sukhodolov *et al.* (2011) implies that the streaks either waver or drift laterally so that a streamwise line of observation alternately crosses high-speed and low-speed streaks.

A simple drawing summarizing these features is presented in Fig. 7. Note that the secondary flows are steady and aligned with the side-walls, and the long streamwise vortices are unsteady

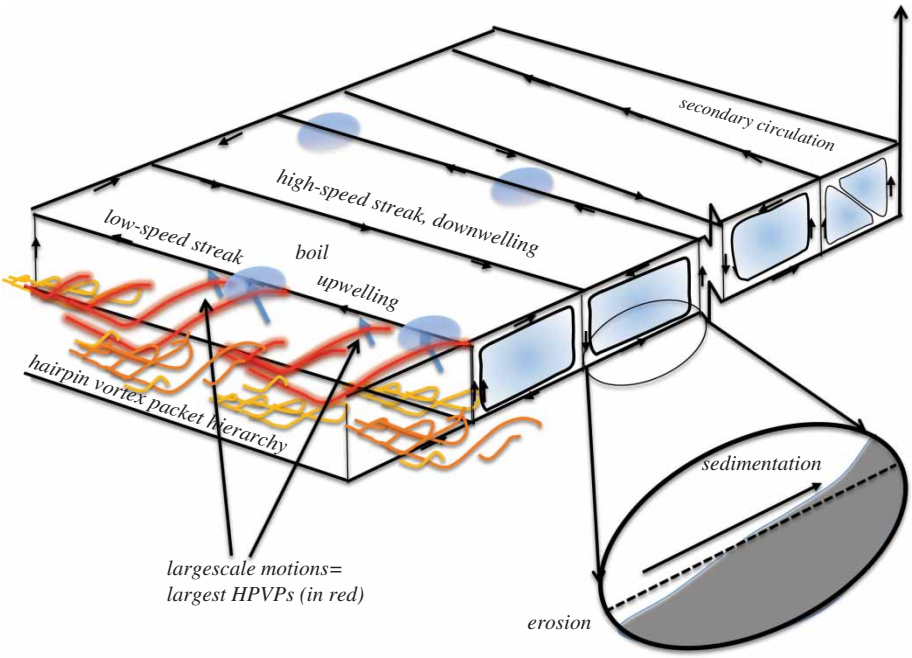

Figure 7 Cartoon of coherent structures in open-channel flows

and inclined. While the cellular picture in Fig. 7 is appealing, the reality of open-channel flows is more complicated. Direct observations of multiple circulations perpendicular to the main channel flow have been made by Nezu (2005), and their instantaneous streamlines clearly fluctuate considerably from cell to cell. Furthermore, the cells do not appear to extend down to the bed. Consequently, the interior cells in Fig. 7 are too regular to represent the instantaneous flow, and the reader should think of them as a conditional average of the roll cells given the location of the centre of the cell as it meanders.

The irregularity of real roll cells can be explained in part by their close association with turbulent "bursts" in the low-speed zones. The term "burst" will be used in the present discussion in deference to common usage in the hydraulics literature. However, there is good evidence that the concept of a burst as a rapid, perhaps even violent, ejection should be replaced by the concept of a packet of hairpin vortices passing and creating a sequence of ejection events, each associated with one of the hairpins. Since the packet evolves relatively slowly, the appearance of rapid change is caused by the fast passage of the packet (Adrian *et al.* 2000). Observations show that a burst can originate at the bed and cross the entire channel depth to impinge on the surface and cause a boil (cf. Shvidchenko and Pender 2001 for a summary of the observations). The bursts reaching the surface have height h, length 2–5h and width 1–2h, virtually the same as the large-scale motions or bulges discussed earlier. In turbulent boundary layers, the bulges are likely to be the ultimate form assumed by the hairpin vortex packets upon reaching the edge of the boundary layer. Consequently, Fig. 7 indicates hairpin vortex packets of various sizes, with the largest (coloured red) causing the surface boils. The smaller packets grow and merge with others to ultimately form the largest packets. PIV measurements in the streamwise vertical plane strongly support the similarity between internal packets in open-channel flow and turbulent boundary layers (Nezu and Sanjou 2011, Fig. 5).

While the association between the low-speed streaks and the succession of bursts that creates "street" of boils is well established, there is a very interesting issue of cause and effect. Shvidchenko and Pender (2001) assert that bursts give rise to the long, streamwise-oriented rolling vortices. But, in their reply to this discussion, Tamburinno and Gulliver note that the rolling vortices may *cause* the ejections and the sweeps, rather than vice versa. A similar idea has been developed independently in the turbulence community. The evidence presented earlier for modulation of the small near-wall scales by the large outer scales supports this picture. The authors' view is that both mechanisms are plausible, and that it is likely that they operate cooperatively. In this scenario, the lateral motion of the cells towards the low-speed streaks sweeps the smaller, growing hairpins and packets into the streaks (Toh and Itano 2005, Adrian 2007) and create the alignment of the LSMs. That alignment creates the VLSMs. Since the hairpins and packets are themselves elements of low momentum, their congregation around the VLSM's low-speed streaks intensifies the momentum deficit. Schoppa and Hussain (2002) have shown that low-speed streaks are necessarily associated with quasi-streamwise roll cells, so intensified low momentum would actually support formation of the roll cells. In this way, a closed-loop feedback cycle would exist in which the roll cells feed themselves by sweeping low-momentum hairpins and packets into the low-speed streaks.

The close relationship between the meandering VLSMs of turbulence structure research and the long cellular motions of open-channel flow research is impossible to ignore. It seems

likely, in fact that they are one and the same. Sukhodolov *et al.* (their Fig. 5b), shows correlation out to 5–10h in a compilation of time delayed streamwise correlation functions from many rivers, and their Fig. 5(a) shows alternating high-speed low-speed zones extending up to free surface. This is very similar to results for meandering VLSMs in pipes, channels and turbulent boundary layers and the atmospheric boundary layer.

5.2 *Structure in channels with significant roughness*

Understanding of coherent structures in rough walled channels is limited, but generally speaking the picture is similar to that for smooth walls, as described in the detailed study by Detert *et al.* (2010). Several observations report structures resembling LSMs that grow up from the wall and reach the surface (Roy *et al.* 2004, Hurther *et al.* 2007, Nikora *et al.* 2007). Surface lengths of 3–5h are reported, but observed widths of 1h are somewhat smaller than the 1–1.5h width of turbulent bulges. It is well known that rough walls reduce the streamwise correlation length. Flow visualization of the bursts from the bed (Roy *et al.* 2004, Fig. 16) shows structures whose growth angle looks similar to the $\sim 15°$ angle of hairpin vortex packets, followed by structures that grow much more rapidly, at least 45°. The latter probably emanates from single roughness elements, and the rapid growth angle offers the simplest explanation for the foreshortening of the streamwise length. The companion paper by Guala *et al.* (2012) offers some insight into the structures created by sparse roughness elements.

5.3 *Heat and mass transfer at the free surface*

Free surface boils and other structures at the surface are hydraulic manifestations of coherent structure rising to the surface. The interactions of the coherent structures with the free surface are also important in the gas exchange at the surface, a major factor in evaluation of greenhouse gas effects. The boils and the upwelling/downwelling streaks are the basis for surface renewal theories, as discussed by Komori *et al.* (1982). In this regard, Calmet and Magnaudet (2003) have shown the significance and utility of Hunt and Graham's (1978) rapid distortion theory for eddies approaching a surface, and this looks like a promising improvement on surface renewal theory.

5.4 *Mixing and dispersion*

Mixing is perhaps one of the most important turbulent processes in problems involving dilution of thermal and material effluents and density stratification in hydraulic flows. Since the importance of coherent structures in the transport of momentum has been established conclusively, it is clear that the transport of heat and mass must also exhibit a strong dependence upon coherent structures. The dispersion of heat and pollutants may be affected by the structure of wall turbulence in shallow channel flows. Jirka (2001) studied wakes, jets and shear layer in wide open channels and noted that three-dimensional turbulent bursts can affect these mainly two-dimensional flows.

Dispersion of scalars is classically modelled as a random walk process that occurs on top of a mean flow field (Sawford 2001, Balachandar and Eaton 2010). The random walk naturally leads to concentration fields caused by dispersion from a point source that are Gaussian functions of position. But in reality, the coherent structures in the flow produce a different picture of the dispersion process. The anisotropy of the structures and their inhomogeneity are factors that are difficult to incorporate realistically into Gaussian models, and the short-term inhomogeneity that is associated with very large-scale superstructures, and their associated large streaks, is almost never accounted for. If the surface were flat and wide, the long streaks would meander with no preferred spanwise location, so that long-time averages would indeed be independent of the spanwise location. But over short times, the streaks tend to stay in one location, causing substantial inhomogeneity. The presence of small-scale inhomogeneity such as rocks, asperities, etc. could cause the streaks to stabilize, meaning that spanwise inhomogeneity would be lost. In such cases, it is very important to model the realizations of the coherent structures rather than their long-time mean values.

5.5 *Erosion and sedimentation*

Erosion and sedimentation often lead to the formation patterns in solid boundaries such as dunes and meanders in streams, and it is, therefore, not unreasonable to look for associations between the formation of these patterns and the coherent patterns of flow in the fluid, at least in the incipient or early stages of erosion when the bed form is essentially flat. Gyr and Schmid (1997) have shown that at incipient erosion on a flat sandy bed, only the sweeps move the sand gains. Erosion processes are also likely to feel the consequences of coherent structures because the low probability, extreme events responsible for high-local erosion rates are parts of the natural cycle of flow. Roughness can also create fluctuation in the wall shear stress that are comparable to the fluctuations caused by coherent structures in smooth-walled flows (Cheng 2006).

When sedimentation and erosion are strong enough to alter the bed form, the coherent structures above the bed may be radically modified, especially by the process of flow separation. For example, Kadota and Nezu (1999) show that the flow behind the crest of a dune is a turbulent shear layer containing spanwise vortices. Nezu *et al.* (1988) and Nezu and Nakagawa (1989b) found that the organized fluid motions and the associated sediment transport occurred intermittently on a movable plane sand bed. After the sand ridges were formed, the roll cells appeared stably across the whole channel cross section. As shown in the inset of Fig. 7, the sand is eroded in the downwelling side of a cell and sedimented on the upwelling side, roll cells are also generated on beds with smooth and rough striping (Nakagawa *et al.* 1981, McLean 1981, Studerus 1982). There is an extensive literature

on the modification of turbulence statistics by various bed form geometries cf. Cellino and Graf (2000). A further comprehensive discussion of coherent structures in sediment dynamics can be found in Garcia (2008).

6 Future challenges and prospects

Our present knowledge of coherent structures in flows over smooth flat surfaces is enough to see how such structures could be of importance in hydraulic engineering. Efforts are needed to exploit understanding of the structure to improve hydraulic engineering design in many areas. Sedimentation, erosion, dispersion and entrance flows to hydraulic devices such as power facilities, spillways and barbs are importantly related to the large-scale and VLSMs, and considerable advancement can be expected if we can adequately characterize and predict these motions and possibly manipulate them in a controlled way. The interactions of the LSMs with the near-wall region, and thus the bed shear stress, also need to be studied and better exploited. Existing predictive models based on the outer region LSMs (Marusic *et al.* 2010b) need to be extended beyond smooth-wall flows and offer the prospect of real predictive capability given only the large-flow field information. Such information can be obtained by reasonably spatially-sparse, low-frequency measurements or preferably from numerical simulations, such as large eddy simulations, where the large flow field information is resolved. Fully understanding the scaling behaviour at high Reynolds numbers also opens the way for refined scale up from models and better-informed designs.

At this point in time the various types of structure have been identified, but one cannot claim that we fully understand their scaling or their functions. Investigations of the scaling of each type of motion are needed. They may provide better definitions of the motions and improve understanding of their relative importance in different ranges of Reynolds number. The interactions of the various motions have only begun to be understood, and much work, especially dynamic experiments and theoretical analyses are needed to establish true cause and effect in these interactions. For example, erosion by VLSMs may be caused by direct action of the VLSMs, but it may also be the case that the very large scales mainly organize and collect the smaller motions, and it is the latter that perform most of the erosion. Understanding cause and effect is essential to management of fluid flows by design.

It would be truly disappointing if improved understanding of the structures in turbulent flows and their roles in sedimentation, erosion and dispersion could not significantly improve the accuracy and reliability of turbulence models of all kinds. Ultimately, incorporation of structural properties into the models is one of the more important and more challenging tasks ahead of the field. It is hoped that improved paradigms of turbulent flow will stimulate new and innovative theoretical descriptions and computational modelling.

The very large Reynolds number inherent to hydraulic flows make them attractive for the study of turbulent structure in the presence of a wide hierarchy of scales and important to turbulent flow science. The wide range of scales across the logarithmic layer would be especially helpful in this regard. The persistence of the logarithmic layer and attached eddies above rough surfaces must be confirmed more fully, as this is an important piece of evidence concerning the robust nature of structures in the outer region. Acquiring such information experimentally will require resolving these flows with an unprecedentedly large dynamic range. However, rapid advances in laser and digital camera technologies combined with evolving three-dimensional velocimetry techniques (Adrian and Westerweel 2011) make this a realistic proposition in the not too distant future.

Acknowledgements

The authors gratefully acknowledge the support of NSF Grant CBET-0933848 (RJA) and the Australian Research Council (IM).

References

Abe, H., Kawamura, H., Choi, H. (2004). Very large-scale structures and their effects on the wall shear–stress fluctuations in a turbulent channel flow up to $R_\tau = 640$. *J. Fluids Eng.* 126(9), 835–843.

Adrian, R.J. (2007). Hairpin vortex organization in wall turbulence. *Phys. Fluids* 19(4), 041301, 1–16.

Adrian, R.J., Meinhart, C.D., Tomkins, C.D. (2000). Vortex organization in the outer region of the turbulent boundary layer. *J. Fluid Mech.* 422, 1–54.

Adrian, R.J., Moin, P. (1988). Stochastic estimation of organized turbulent structure: Homogeneous shear flow. *J. Fluid Mech.* 190, 531–559.

Adrian, R.J., Westerweel, J. (2011). *Particle image velocimetry.* Cambridge University Press, Cambridge, UK.

Alfredsson, P.H., Johansson, A.V., Haritonidis, J.H., Eckelmann, H. (1988). The fluctuating wall-shear stress and the velocity-field in the viscous sublayer. *Phys. Fluids* 31(5), 1026–1033.

Balachandar, S., Eaton, J.K. (2010). Turbulent dispersed multiphase flow. *Ann. Rev. Fluid Mech.* 42, 111–133.

Balakumar, B.J., Adrian, R.J. (2007). Large- and very-large-scale motions in channel and boundary-layer flows. *Philos. Trans. R. Soc. Lond. A* 365, 665–681.

Bandyopadhyay, P.R. (1980). Large structure with a characteristic upstream interface in turbulent boundary layers, *Phys. Fluids* 23, 2326–1980.

Barenblatt, G.I. (1993). Scaling laws for fully developed turbulent shear flows. Part 1. Basic hypotheses and analysis. *J. Fluid Mech.* 248, 513–520.

Blackwelder, R.F., Kaplan, R.E. (1976). On the wall structure of the turbulent boundary layer. *J. Fluid Mech*. 76, 89–112.

Blackwelder, R.F., Kovasznay, L.S.G. (1972). Time scales and correlations in a turbulent boundary layer. *Phys. Fluids* 15, 1545–1554.

Bogard, D.G., Tiederman, W.G. (1986). Burst detection with single-point velocity measurements. *J. Fluid Mech.* 162, 389–413.

Brodkey, R.S., Wallace, J.M., Eckelmann, H. (1974). Some properties of truncated turbulence signals in bounded shear flows. *J. Fluid Mech.* 63, 209–224.

Calmet, I., Magnaudet, J. (2003). Statistical structure of high-Reynolds-number turbulence close to the free surface of an open-channel flow. *J. Fluid Mech*. 474, 355–378.

Cantwell, B.J. (1981). Organized motion in turbulent flow. *Ann. Rev. Fluid Mech.* 13, 457–515.

Carlier, J., Stanislas, M. (2005). Experimental study of eddy structures in a turbulent boundary layer using particle image velocimetry. *J. Fluid Mech.* 535, 143–188.

Cellino, M., Graf, W.H. (2000). Experiments on suspension flow in open channels with bed forms. *J. Hydraulic Res.* 38(4), 289–298.

Cheng, N. (2006). Influence of shear stress fluctuation on bed particle mobility. *Phys. Fluids* 18(9), 096602, 1–7.

Coles, D.E. (1956). The law of the wake in the turbulent boundary layer. *J. Fluid Mech.* 1, 191–226.

Dennis, D.J.C., Nickels, T.B. (2008). On the limitations of taylor's hypothesis in constructing long structures in a turbulent boundary layer. *J. Fluid Mech.* 614, 197–206.

Dennis, D.J.C., Nickels, T.B. (2011a). Experimental measurement of large-scale three-dimensional structures in a turbulent boundary layer. Part 1: Vortex packets. *J. Fluid Mech.* 673, 180–217.

Dennis, D.J.C., Nickels, T.B. (2011b). Experimental measurement of large scale three-dimensional structures in a turbulent boundary layer. Part 2: Long structures. *J. Fluid Mech.* 673, 218–244.

DeGraaff, D.B., Eaton, J.K. (2000). Reynolds-number scaling of the flat-plate turbulent boundary layer. *J. Fluid Mech.* 422, 319–346.

Detert, M., Nikora, V., Jirka, G.H. (2010). Synoptic velocity and pressure fields at the water–sediment interface of streambeds. *J. Fluid Mech.* 660, 55–86.

Ganapathisubramani, B., Hutchins, N., Hambleton, W.T., Longmire, E.K., Marusic, I. (2005). Investigation of large-scale coherence in a turbulent boundary layer using two-point correlations. *J. Fluid Mech.* 524, 57–80.

Ganapathisubramani, B., Longmire, E.K., Marusic, I. (2003). Characteristics of vortex packets in turbulent boundary layers. *J. Fluid Mech.* 478, 35–46.

Garcia, G. (2008). Sediment transport and morphodynamics. In Sedimentation engineering: Processes, measurements, modeling, and practice, 21–164, M. Garcia, ed. American Society of Civil Engineers, Manuals and Reports on Engineering Practice 110. Reston, Virginia.

George, W.K., Castillo, L. (1997). Zero-pressure-gradient turbulent boundary layer. *App. Mech. Rev*. 50(12), 689–729.

Grant, S.B., Marusic, I. (2011). Crossing turbulent boundaries: Interfacial flux in environmental flows. *Environ. Sci. Technol.* 45(17), 7107–7113.

Grinvald, D., Nikora, V. (1988). *River Turbulence (Rechnaya turbulentnosti)* (in Russian). Hydrometeoizdat, Russia.

Guala, M., Tomkins, C.D., Christiansen, K.T., Adrian, R.J. (2012). Vortex organization in turbulent boundary layer flow over sparse roughness elements. *J. Hydraulic Res.* 50(5), 465–481.

Gulliver, J.S., Halverson, M.J. (1987). Measurements of large streamwise vortices in an open-channel flow. *Water Resour. Res.* 23(1), 115–123.

Guezennec, Y.G., Piomelli, U., Kim, J. (1989). On the shape and dynamics of wall structures in turbulent channel flow. *Phys Fluids A* 1(4), 764–766.

Gyr, A., Schmid, A. (1997) Turbulent flows over smooth erodible sand beds in flumes. *J. Hydraulic Res.* 35, 525–544.

Hambleton, W.T., Hutchins, N., Marusic, I. (2006). Simultaneous orthogonal-plane particle image velocimetry measurements in a turbulent boundary layer. *J. Fluid Mech.* 560, 53–64.

Head, M.R., Bandyopadhyay, P.R. (1981). New aspects of turbulent boundary-layer structure. *J. Fluid Mech.* 107, 297–337.

Hommema, S.E., Adrian, R.J. (2003). Packet structure of surface eddies in the atmospheric boundary layer. *Boundary-Layer Meterorol.* 106, 147–170.

Hoyas, S., Jimenez, J. (2006). Scaling of the velocity fluctuations in turbulent channels up to $\mathsf{R}_\tau = 2003$. *Phys. Fluids* 18(1), 011702, 1–4.

Hunt, J.C.R., Graham, J.M.R. (1978). Free stream turbulence near plane boundaries. *J. Fluid Mech.* 84, 209–235.

Hunt, J.C.R., Morrison, J.F. (2000). Eddy structure in turbulent boundary layers. *Eur. J. Mech. B-Fluids* 19, 673–694.

Hurther, D., Lemmin, U., Terray, E.A. (2007). Turbulent transport in the outer region of rough-wall open-channel flows: The contribution of large coherent shear stress structures (LC3S). *J. Fluid Mech.* 574, 465–493.

Hutchins, N., Marusic, I. (2007a). Evidence of very long meandering streamwise structures in the logarithmic region of turbulent boundary layers. *J. Fluid Mech.* 579, 1–28.

Hutchins, N., Marusic, I. (2007b). Large-scale influences in near-wall turbulence. *Philos. Trans. R. Soc. Lond. A* 365, 647–664.

Hutchins, N., Chauhan, K., Marusic, I., Monty, J., Klewicki, J. (2012, in press). Towards reconciling the large-scale structure of turbulent boundary layers in the atmosphere and laboratory. *Boundary-Layer Meterol.*

Hussain, A.K.M.F. (1986). Coherent structures and turbulence. *J. Fluid Mech.* 173, 303–356.

Imamoto, H., Ishigaki, T. (1986). Visualization of longitudinal eddies in an open-channel flow. Proc. 4th Int. Symp. *Flow Visualization*, 333–337, C. Veret, ed. Hemisphere, Washington, DC.

Jimenez, J. (2004). Turbulent flows over rough walls. *Annu. Rev. Fluid Mech.* 36, 173–96.

Jimenez, J. (2012). Cascades in wall-bounded turbulence. *Ann. Rev. Fluid Mech.* 44, 27–45.

Jirka, G.H. (2001). Large scale flow structures and mixing processes in shallow flows. *J. Hydraulic Res.* 39(6), 567–573.

Kadota, A., Nezu, I. (1999). Three-dimensional structure of space-time correlation on coherent vortices generated behind dune crest, *J. Hydraulic Res.* 37(1), 59–80.

Kim, J. (1987). Evolution of a vortical structure associated with the bursting event in a channel flow. In *Turbulent shear flows* 5, F. Durst, B.E. Launder, J.L. Lumley, F.W. Schmidt, J.H. Whitelaw, eds. Springer-Verlag, New York. pp. 221–227.

Kim, K.C., Adrian, R.J. (1999). Very large-scale motion in the outer layer. *Phys. Fluids* 11(2), 417–422.

Klaven, A.B., Kopaliani, Z.D. (1973). *Laboratory investigations of kinematic structure of turbulent flow over a very rough bed* (in Russian). Tarns. State Hydro. Inst. Gidrometeoizdat, Leningrad, Russia.

Kline, S.J. (1978). The role of visualization in the study of the structure of the turbulent boundary layer. *Lehigh workshop on coherent structure of turbulent boundary layers*, C.R. Smith, D.E. Abbott, eds. 1–26. Lehigh University, USA.

Kline, S.J., Reynolds, W.C., Schraub, F.A., and Rundstadler, P.W. (1967). The structure of turbulent boundary layers. *J. Fluid Mech.* 30, 741–773.

Komori, S., Ueda, H., Ogino, F., Mizushina, T. (1982). Turbulence structure and transport mechanism at the free surface in an open channel flow. *Int. J. Heat Mass Trans.* 25(4), 513–521.

Kovasznay, L.S.G., Kibens, V., Blackwelder, R.F. (1970). Large scale motion in the intermittent region of a turbulent boundary layer. *J. Fluid Mech.* 41, 283–325.

Liu, Z.C., Adrian, R.J., Hanratty, T.J. (1991). High resolution measurement of turbulent structure in a channel with particle image velocimetry. *Exp. Fluids* 10(6), 301–312.

Luchik, T.S., Tiederman,W.G. (1987). Time-scale and structure of ejections and bursts in turbulent channel flows. *J. Fluid Mech.* 174, 529–552.

Marusic, I., Adrian, R.J. (2013). Eddies and scales of wall turbulence. In *Ten chapters in turbulence*, P.A. Davidson, Y. Kaneda, K.R. Sreenivasan, eds. Cambridge University Press, Cambridge, UK.

Marusic, I., Mathis, R., Hutchins, N. (2010a). Predictive model for wall-bounded turbulent flow. *Science* 329 (5988), 193–196.

Marusic, I., Mathis, R., Hutchins, N. (2011). A wall-shear stress predictive model. *J. Phys. Conf. Ser.* 318, 012003, 1–8.

Marusic, I., McKeon, B.J., Monkewitz, P.A., Nagib, H.M., Smits, A.J., Sreenivasan, K.R. (2010b). Wall-bounded turbulent flows: Recent advances and key issues. *Phys. Fluids* 22(6), 065103, 1–24.

Mathis, R., Hutchins, N., Marusic, I. (2009). Large-scale amplitude modulation of the small-scale structures in turbulent boundary layers. *J. Fluid Mech.* 628, 311–337.

Metzger, M.M., Klewicki, J.C. (2001). A comparative study of near-wall turbulence in high and low Reynolds number boundary layers. *Phys. Fluids* 13(3), 692–701.

Monty, J.P., Hutchins, N., Ng, H.C.H., Marusic, I., Chong, M.S. (2009). A comparison of turbulent pipe, channel and boundary layer flows. *J. Fluid Mech.* 632, 431–442.

Monty, J.P., Stewart, J.A., Williams, R.C., Chong, M.S. (2007). Large-scale features in turbulent pipe and channel flows. *J. Fluid Mech.* 589, 147–156.

Nagib, H.M., Chauhan K.A., Monkewitz P.A. (2007). Approach to an asymptotic state for zero pressure gradient turbulent boundary layers. *Philos. Trans. R. Soc. Lond. A.* 365, 755–770.

Nakagawa, H., Nezu, I., Tominaga, A. (1981). Turbulent structure with and without cellular secondary currents over various bed configurations. *Annu, DPRI*, Kyoto Univ., 24B, 315–338 in Japanese.

Nezu, I. (2005). Open-channel flow turbulence and its research prospect in the 21st century. *J. Hydraulic Eng.* 131(4), 229–246.

Nezu, I., Nakagawa, H. (1993). *Turbulence in open-channel flows*. IAHR-Monograph, Balkema, Rotterdam, The Netherlands.

Nezu, I., Nakayama T. (1997). Space-time correlation structures of horizontal coherent vortices in compound open-channel flows by using particle tracking velocimetry. *J. Hydraulic Res.* 35(2), 191–208.

Nezu, I., Nakagawa, H., Kawashima, N. (1988). Cellular secondary currents and sand ribbons in fluvial channel flows. Proc. *6th APDIAHR Congress*, Vol. 1, Delft, The Netherlands, 51–58.

Nezu, I., Nakagawa, H. (1989). Self forming mechanism of longitudinal sand ridges and troughs. Proc. *23rd IAHR Congress*, Vol. B, IAHR, Delft, The Netherlands, 65–72.

Nezu, I., Rodi, W. (1986). Open-channel flow measurements with a laser Doppler anemometer. *J. Hydraulic Eng.* 112, 335–355.

Nezu, I., Sanjou, M. (2011). PIV and PTV measurements in hydro-sciences with focus on turbulent open-channel flows. *J. Hydro-environment Res.* 5(4), 215–230.

Nikora, V., Nokes, R., Veale, W., Davidson, M., Jirka, G.H. (2007). Large-scale turbulent structure of uniform shallow free-surface flows. *Environ. Fluid Mech.* 7(2), 159–172.

Nikora, V. (2010). Hydrodynamics of aquatic ecosystems: An interface between ecology, biomechanics and environmental fluid mechanics. *River Res. Applic.* 26(4), 367–384.

Nikora, V., Roy, A.G. (2012). Secondary flows in rivers: Theoretical framework, recent advances, and current challenges. In *Gravel-bed Rivers: Processes, Tools, Environments*. M. Church, P.M. Biron, A.G. Roy, eds. John Wiley & Sons, USA, 3–22.

Onitsuka, K., Nezu, I. (2001). Generation mechanism of turbulence driven secondary currents in open-channel flows. IUTAM Symp. *Geometry and statistics of turbulence*,

345–350, K. Kambe, T. Nakano, T. Miyauchi, eds., Kluwer Academic, Boston.

Orlu, R., Schlatter, P. (2011). On the fluctuating wall-shear stress in zero-pressure-gradient turbulent boundary layers. *Phys. Fluids* 23(2), 021704, 1–4.

Panton, R.L. (2001). Overview of the self-sustaining mechanisms of wall turbulence. *Prog. Aerosp. Sci.* 37, 341–383.

Perry, A.E., Chong, M.S. (1982). On the mechanism of wall turbulence. *J. Fluid Mech.* 119, 173–217.

Perry, A.E., Henbest, S.M., Chong, M.S. (1986). A theoretical and experimental study of wall turbulence. *J. Fluid Mech.* 165, 163–199.

Perry, A.E., Marusic, I. (1995). A wall-wake model for the turbulence structure of boundary layers Part 1. Extension of the attached eddy hypothesis. *J. Fluid Mech.* 298, 361–388.

Rao, K.N., Narasimha, R., Badri Narayanan, M.A. (1971). The 'bursting' phenomena in a turbulent boundary layer. *J. Fluid Mech.* 48, 339–352.

Robinson, S.K. (1991). Coherent motions in turbulent boundary layers. *Ann. Rev. Fluid Mech.* 23, 601–639.

Rodriguez, J.F., Garcia, M.H. (2008). Laboratory measurements of 3-D flow patterns and turbulence in straight open channel with rough bed. *J. Hydraulic Res.* 46(4), 454–465.

Rogers, M.M., Moin, P. (1987). The structure of the vorticity field in homogeneous turbulent flows. *J. Fluid Mech.* 176, 33–66.

Roy, A.G., Langer, T.B., Lamarre, H., Kirkbride, A.D. (2004). Size, shape and dynamics of large-scale turbulent flow structures in a gravel-bed river. *J. Fluid Mech.* 500, 1–27.

Sawford, B. (2001). Turbulent relative dispersion. *Ann. Rev. Fluid Mech.* 33, 289–317.

Schoppa, W., Hussain, F. (2002). Coherent structure generation in near-wall turbulence. *J. Fluid Mech.* 453, 57–108.

Shvidchenko, A.B., Pender, G. (2001). Large flow structures in a turbulent open channel flow. *J. Hydraulic Res.* 39(1), 109–111.

Smith, C.R. (1984). A synthesized model of the near-wall behavior in turbulent boundary layers. Proc. 8th Symp. *Turbulence*, 299–325, J. Zakin, G. Patterson, eds., University of Missouri-Rolla.

Smits, A.J., McKeon, B.J., Marusic, I. (2011). High Reynolds number wall turbulence. *Ann. Rev. Fluid Mech.* 43, 353–375.

Sukhodolov, A.N., Nikora, V.I., Katolokov, V.M. (2011). Flow dynamics in alluvial channels: the legacy of Kirill V. Grishanin. *J. Hydraulic Res.* 49, 285–292.

Tamburrino, A., Gulliver, J.S. (1999). Large flow structures in a turbulent open channel flow. *J. Hydraulic Res*. 37, 363–380.

Tamburrino, A., Gulliver, J.S. (2007). Free-surface visualization of streamwise vortices in a channel flow. *Water Resour. Res.* 43, W11410, 1–12.

Tardu, S. (1995). Characteristics of single and clusters of bursting events in the inner layer, Part 1: Vita events. *Exps Fluids* 20, 112–124.

Theodorsen, T. (1952). Mechanism of turbulence. Proc. 2nd Midwest. Conf. *Fluid Mechanics*, March 17–19, 1–19, Ohio State University, Columbus.

Toh, S., Itano, T. (2005). Interaction between a large-scale structure and near-wall structures in channel flow. *J. Fluid Mech.* 524, 249–262.

Tomkins, C.D., Adrian, R.J. (2005). Energetic spanwise modes in the logarithmic layer of a turbulent boundary layer. *J. Fluid Mech.* 545, 141–162.

Townsend, A.A. (1976). *The structure of turbulent shear flow*. Cambridge University Press, Cambridge, UK.

Velikaniv, M.A. (1958). *Channel processes* (in Russian). Fismatgiz, Moscow.

Wallace, J.M., Eckelmann, H., Brodkey, R.S. (1972). The wall region in turbulent shear flow. *J. Fluid Mech.* 54, 39–48.

Wark, C.E., Nagib, H.M. (1991). Experimental investigation of coherent structures in turbulent boundary layers. *J. Fluid Mech.* 230, 183–208.

Willmarth, W.W., Lu, S.S. (1972). Structure of the Reynolds stress near the wall. *J. Fluid Mech.* 55, 65–92.

Yalin, M.S. (1992). *River mechanics*. Pergamon Press, Oxford, UK.

Zagarola, M.V., Smits, A.J. (1998). An-flow scaling of turbulent pipe flow. *J. Fluid Mech.* 373, 33–79.